

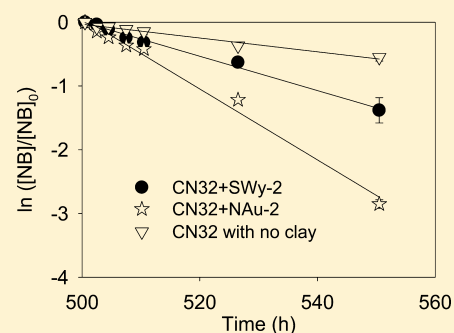
## 1 Iron(III)-Bearing Clay Minerals Enhance Bioreduction of Nitrobenzene 2 by *Shewanella putrefaciens* CN32

3 Fubo Luan, Yan Liu, Aron M. Griffin, Christopher A. Gorski, and William D. Burgos\*

4 Department of Civil and Environmental Engineering, The Pennsylvania State University, University Park, Pennsylvania 16801-1408,  
5 United States

6 **S** Supporting Information

7 **ABSTRACT:** Iron-bearing clay minerals are ubiquitous in the environment, and  
8 the clay-Fe(II)/Fe(III) redox couple plays important roles in abiotic reduction  
9 of several classes of environmental contaminants. We investigated the role of  
10 Fe-bearing clay minerals on the bioreduction of nitrobenzene. In experiments  
11 with *Shewanella putrefaciens* CN32 and excess electron donor, we found that the  
12 Fe-bearing clay minerals montmorillonite SWy-2 and nontronite NAu-2 enhanced  
13 nitrobenzene bioreduction. On short time scales (<50 h), nitrobenzene reduction  
14 was primarily biologically driven, but at later time points, nitrobenzene reduction  
15 by biologically formed structural Fe(II) in the clay minerals became increasingly  
16 important. We found that chemically reduced (dithionite) iron-bearing clay  
17 minerals reduced nitrobenzene more rapidly than biologically reduced iron-bearing  
18 clay minerals despite the minerals having similar structural Fe(II) concentrations.  
19 We also found that chemically reduced NAu-2 reduced nitrobenzene faster as compared to chemically reduced SWy-2. The  
20 different reactivity of SWy-2 versus NAu-2 toward nitrobenzene was caused by different forms of structural clay-Fe(II) in the clay  
21 minerals and different reduction potentials ( $E_h$ ) of the clay minerals. Because most contaminated aquifers become reduced via  
22 biological activity, the reactivity of biogenic clay-Fe(II) toward reducible contaminants is particularly important.



### 23 ■ INTRODUCTION

24 Iron-bearing clay minerals are widely distributed in nature and  
25 have been estimated to account for up to 50% of the Fe in soils  
26 and sediments.<sup>1–3</sup> Much of the structural Fe in clay minerals  
27 can participate in redox reactions,<sup>4</sup> and the Fe(II)/Fe(III)  
28 redox couple is thought to be an important redox buffer  
29 across a wide range of redox conditions.<sup>5–16</sup> Structural Fe(II) in  
30 clay minerals is also important from an environmental  
31 perspective since it can reduce a wide range of contaminants,  
32 including toxic metals,<sup>17,18</sup> radionuclides,<sup>19–21</sup> nitroaromatic  
33 explosives,<sup>22–24</sup> and chlorinated solvents,<sup>25</sup> altering their fate  
34 and mobility. Structural Fe(III) in clay minerals can be reduced  
35 both abiotically, for instance by dissolved Fe(II), sulfide,  
36 and reduced natural organic matter,<sup>26,27</sup> and biotically by  
37 several types of naturally occurring metal- and sulfate-reducing  
38 microorganisms.<sup>28,29</sup>

39 Nitroaromatic compounds (NACs) are ubiquitous environ-  
40 mental contaminants. Understanding the environmental fate  
41 of NACs is of great interest due to their mutagenic and  
42 carcinogenic effects.<sup>30,31</sup>

43 The abiotic reduction of NACs by chemically reduced iron-  
44 bearing clay minerals has been well studied.<sup>22–24</sup> Several types  
45 of dissimilatory metal-reducing bacteria (DMRB) can reduce  
46 both NACs<sup>32,33</sup> and iron-bearing clay minerals.<sup>34,35</sup> As noted  
47 in a recent review, what remained unclear was if and how  
48 iron-bearing clay minerals would influence the bioreduction of  
49 NACs by DMRB.<sup>36</sup> In these systems, clay-Fe(III) reduction  
50 may compete with NAC reduction for available electron donor,

and/or produce biogenic structural clay-Fe(II) that serves as a  
51 reductant of the NAC. 52

In previous work, we examined interactions between hematite,  
53 nitrobenzene, and *Shewanella putrefaciens* CN32, a DMRB  
54 capable of using both hematite and nitrobenzene as terminal  
55 electron acceptors.<sup>32</sup> In that system, Fe(II)-mediated reduction  
56 of nitrobenzene enhanced the rate of nitrobenzene reduction.  
57 However, nitrobenzene reduction occurred primarily by direct  
58 respiration by DMRB on short time scales (<24 h). We suggested  
59 that Fe(II)-mediated reduction by iron oxides would become a  
60 more important role on bioreduction of nitrobenzene in long-  
61 term experiments. Iron-bearing clay minerals differ from iron  
62 oxides in many ways.<sup>37,38</sup> Importantly, the content and structural  
63 locations of iron in clay minerals are distinct from oxides.  
64 Additionally, the reduction of iron-bearing clay minerals is not  
65 subject to reductive dissolution to the same extent as with  
66 iron oxides.<sup>39</sup> Therefore, we were interested in the interactions  
67 between iron-bearing clay minerals, DMRB, and nitrobenzene.  
68 We anticipated that our new findings would differ from previous  
69 work done with iron oxides, and purposefully conducted long-  
70 term experiments to differentiate short-term and long-term effects.  
71

Many studies examining contaminant reduction by structural  
72 Fe(II) in clay minerals use chemically reduced specimens.<sup>22–24</sup> 73

Received: August 23, 2014

Revised: January 3, 2015

Accepted: January 6, 2015

74 Fe(III)-bearing clay minerals reduced by microorganisms  
75 versus chemical reductants yield products that are different  
76 with respect to their spectroscopic properties.<sup>40</sup> This has led to  
77 the suggestion that bacteria and commonly used chemical  
78 reductants reduce structural Fe(III) via different reaction  
79 mechanisms, and that the clay-microbe interactions may involve  
80 more than just electron transfer.<sup>40</sup> To date, we know of no  
81 studies that have compared the reactivity of biologically  
82 reduced versus chemically reduced iron-bearing clay minerals  
83 with NACs. Such knowledge is particularly important to the  
84 natural attenuation of NACs.

85 In the current work, we examined the role of iron-bearing  
86 clay minerals on the bioreduction of NACs by DMRB. To  
87 study these interactions, we (i) used nitrobenzene as a model  
88 NAC contaminant since it has been used extensively in the  
89 past to probe the reductive capabilities of Fe(II)-bearing clay  
90 minerals in abiotic systems;<sup>22–24</sup> (ii) selected montmorillonite  
91 SWy-2 (0.40 mmol Fe/g) and nontronite NAu-2 (4.1 mmol  
92 Fe/g) as two model clay minerals because they represent  
93 smectite end-members with respect to Fe content<sup>20</sup>; and (iii)  
94 chose *Shewanella putrefaciens* CN32 as a model Fe-reducing  
95 bacterium since it can respire on both clay-Fe(III) and  
96 nitrobenzene. In long-term bioreduction experiments, nitro-  
97 benzene was respiked into the batch reactors multiple times to  
98 gauge the importance of biotic versus abiotic nitrobenzene  
99 reduction with increasing concentrations of clay-Fe(II). Abiotic  
100 nitrobenzene reduction experiments were also conducted with  
101 biologically reduced (and pasteurized) and chemically reduced  
102 clay minerals to examine how the Fe(III) reduction pathway  
103 influenced the reactivity of clay-Fe(II).

## 104 ■ MATERIALS AND METHODS

105 **Microorganism and Culture Conditions.** *Shewanella*  
106 *putrefaciens* strain CN32 was grown aerobically on tryptic  
107 soy broth without dextrose (Difco) at 20 °C, and cells were  
108 harvested and prepared anaerobically as previously described.<sup>32,41</sup>

109 **Minerals and Chemicals.** Both nontronite NAu-2 and  
110 montmorillonite SWy-2 were purchased from the source clays  
111 repository of the Clay Minerals Society (West Lafayette, IN).  
112 The solid-phase mineral compositions of NAu-2<sup>42</sup> and SWy-2<sup>20</sup>  
113 have previously been reported as

114 NAu-2:  $M^{+}_{0.72}[\text{Si}_{7.55}\text{Al}_{0.16}\text{Fe}_{0.29}][\text{Al}_{0.34}\text{Fe}_{3.54}\text{Mg}_{0.05}]\text{O}_{20}(\text{OH})_4$ ,  
115 where M may be Ca, Na or K

116 SWy-2:  $(\text{Ca}_{0.16}\text{Na}_{0.24})[\text{Si}_{6.73}\text{Al}_{1.27}][\text{Al}_{1.45}\text{Fe}^{2+}_{0.01}\text{Fe}^{3+}_{0.12}\text{Mg}_{0.44}]-$   
117  $\text{O}_{20}(\text{OH})_4$

118 NAu-2 and SWy-2 were suspended in 0.5 M NaCl for 24 h,  
119 then separated by centrifugation, yielding the 0.5–2.0 μm clay  
120 size fraction. The clay fraction was washed with distilled  
121 deionized water (Milli-Q) repeatedly until no Cl<sup>-</sup> was detected  
122 by silver nitrate and then dried at 60 °C. Based on an anoxic  
123 HF-H<sub>2</sub>SO<sub>4</sub>/phenanthroline digestion,<sup>43</sup> the NAu-2 clay fraction  
124 contained 4.1 mmol of Fe/g clay and 99.4% Fe(III), while the  
125 SWy-2 clay fraction contained 0.40 mmol of Fe/g clay and  
126 97.3% Fe(III). NAu-2 and SWy-2 clay fraction stock solutions  
127 (20 g L<sup>-1</sup>) were prepared in anoxic 10 mM PIPES [piperazine-  
128 N,N'-bis(2-ethanesulfonic acid), pK<sub>a</sub> = 6.8] buffer adjusted to  
129 pH 6.8. Aluminum oxide (Al<sub>2</sub>O<sub>3</sub>) was used as a redox-inactive  
130 mineral control and its stock solution (20 g L<sup>-1</sup>) was prepared  
131 in anoxic 10 mM PIPES buffer (pH 6.8).

132 Reagent grade nitrobenzene (Sigma-Aldrich), nitrosobenzene  
133 (TCI America), phenylhydroxylamine (Sigma-Aldrich), and aniline  
134 (Sigma-Aldrich) were used to prepare 0.16 M stock solutions in  
135 methanol.

**Bioreduction of Iron(III)-Bearing Clay Minerals and** 136  
**Nitrobenzene.** All experiments were conducted in 30 mL 137  
serum bottles crimp-sealed with Teflon-faced rubber stoppers. 138  
All preparations were performed in an anoxic chamber 139  
(Coy, Grass Lakes, MI) supplied with a 95:5 N<sub>2</sub>:H<sub>2</sub> gas mix. 140  
The anoxic chamber (<1 ppm, O<sub>2</sub>) was in a 20 °C constant- 141  
temperature room. Reactors were filled with ~20 mL of 142  
deoxygenated 10 mM PIPES buffer (pH 6.8) containing various 143  
combinations of CN32 (1 × 10<sup>8</sup> cell/mL), NAu-2 or SWy-2 or 144  
Al<sub>2</sub>O<sub>3</sub> (2.0 g/L), and nitrobenzene (210 μM). Ten mM sodium 145  
lactate was provided as the electron donor for bioreduc- 146  
tion experiments, a concentration high enough to reduce 147  
all the nitrobenzene and all the clay-Fe(III) in any experiment. 148  
Long-term experiments were conducted where nitrobenzene 149  
was respiked into the reactors (250 μM) at 45 and 500 h. 150  
Nitrobenzene concentrations were always less than 25 μM 151  
before nitrobenzene was respiked. Control reactors were 152  
prepared containing only nitrobenzene and buffer. Other sets 153  
of control reactors were prepared with CN32 and NAu-2 but 154  
without nitrobenzene plus 0.25% methanol (vol/vol %; to 155  
account for cosolvent addition) or nitrosobenzene (210 μM) or 156  
aniline (210 μM). Nitrosobenzene and aniline were included to 157  
examine the effects of nitrobenzene metabolites on clay-Fe(II) 158  
production. Methanol and aniline were shown to have no effect 159  
on clay-Fe(II) production (SI Figure S1). All treatments and 160  
controls were run in triplicate. Reactors were incubated at 161  
100 rpm on orbital shakers within the anoxic chamber. After 162  
cell inoculation, samples were periodically removed with sterile 163  
needles and syringes. Samples were analyzed for soluble Fe(II), 164  
clay-Fe(II), and nitrobenzene and its metabolites as described 165  
below. All sampling and Fe(II) measurements were performed 166  
in the anoxic chamber. 167

**Abiotic Reduction of Nitrobenzene by Reduced** 168  
**Iron(III)-Bearing Clay Minerals.** Bioreduced clay minerals 169  
were prepared using CN32 and NAu-2 or SWy-2 (with no 170  
nitrobenzene) as described above. Reactors were incubated for 171  
900 h, at which point the biogenic clay-Fe(II) concentration 172  
essentially stopped increasing. Cell-clay mineral suspensions 173  
were washed 3 times with anoxic 50 mM PIPES buffer (pH 6.8) 174  
to remove residual sodium lactate and were then pasteurized 175  
(75 °C for 60 min, three times over 5 days) to deactivate bio- 176  
logical activity. No further attempt was made to remove spent 177  
biomass. The bioreduced clay minerals were prepared as stock 178  
solutions (20 g/L) in anoxic 50 mM PIPES buffer. 179

NAu-2 and SWy-2 were chemically reduced using sodium 180  
dithionite (6 g/L) in a sodium citrate (266 mM)/sodium 181  
bicarbonate (111 mM) buffer (CBD method).<sup>44,45</sup> These lower 182  
concentrations of dithionite and shorter reaction periods 183  
were used to produce partially reduced NAu-2. The chemically 184  
reduced clay minerals were washed 3 times with anoxic sodium 185  
citrate/sodium bicarbonate buffer and 3 times with anoxic 50 mM 186  
PIPES buffer to remove residual dithionite. Stock solutions 187  
(20 g/L) were prepared in anoxic 50 mM PIPES buffer. 188

Abiotic reduction of nitrobenzene was conducted with 189  
biologically reduced (and pasteurized) and chemically reduced 190  
clay minerals. Clay mineral suspension concentrations (g clay L<sup>-1</sup>) 191  
were varied such that experiments began with equal clay-Fe(II) 192  
concentrations. For NAu-2, depending on the clay-Fe(III) 193  
reduction extent, clay suspension concentrations varied from 194  
1.1 to 5.3 g L<sup>-1</sup> and initial clay-Fe(II) concentrations ranged 195  
from 1.1 to 5.3 mM Fe(II). For SWy-2, clay suspension 196  
concentrations varied from 3.1 to 3.6 g L<sup>-1</sup> and clay-Fe(II) 197  
concentrations ranged from 1.1 to 1.3 mM Fe(II). Nitrobenzene 198

199 was always added at a constant concentration of 250  $\mu\text{M}$ . All  
200 treatments and controls were run in triplicate. Reactors were  
201 incubated at 100 rpm on orbital shakers within the anoxic  
202 chamber. Samples were periodically removed with sterile needles  
203 and syringes and analyzed for clay-Fe(II) and nitrobenzene as  
204 described below. Sample suspensions were centrifuged at  
205 14 100g for 10 min (pelletized particles  $<0.02 \mu\text{m}$ ) in the anoxic  
206 chamber. The supernatant was used to measure soluble Fe(II),  
207 nitrobenzene, nitrosobenzene, and aniline.

208 **Analytical Methods.** Nitrobenzene, nitrosobenzene,  
209 phenylhydroxylamine, and aniline were measured by an HPLC  
210 equipped with a C18 column and photodiode array detector  
211 using an methanol/water (1/1, v/v) mobile phase. Soluble  
212 Fe(II) was measured using the phenanthroline method.<sup>46</sup> The  
213 mineral pellet was used to measure the clay-Fe(II) concentra-  
214 tion using a modified anoxic HF-H<sub>2</sub>SO<sub>4</sub>/phenanthroline digestion  
215 method.<sup>43</sup> Total clay-Fe(II) was calculated as the sum of the  
216 soluble Fe(II) plus HF-H<sub>2</sub>SO<sub>4</sub>/phenanthroline Fe(II).

217 **Mössbauer Spectroscopy.** Transmission Mössbauer spec-  
218 troscopy was performed using a SVT400 cryogenic Mössbauer  
219 system (SEE Co.). The <sup>57</sup>Co ( $\sim 50 \text{ mCi}$ ) was in a Rh matrix at  
220 room temperature. All hyperfine parameters were reported  
221 relative to  $\alpha$ -Fe foil at room temperature. Clay mineral wet  
222 pastes were prepared anaerobically and sealed between two  
223 pieces of 5 mL kapton tape to avoid oxidation when the sample  
224 was transferred from the anoxic chamber to the sample  
225 holder. Spectral fitting was conducted using Recoil Software  
226 (University of Ottawa, Ottawa, Canada). All fits were done  
227 using a Voigt-based model. The Lorentzian line width was held  
228 at 0.14 mm s<sup>-1</sup> during fitting, as it was the line width measured  
229 on the spectrometer for an ideally thick  $\alpha$ -Fe foil. For all fits,  
230 unless otherwise noted, the center shift (CS), quadrupole shift  
231 (QS), and relative areas between sites were allowed to float  
232 during fitting.

233 **Kinetic Analyses.** The rate of nitrobenzene reduction by  
234 CN32 or clay-Fe(II) was modeled as pseudo-first-order with  
235 respect to the nitrobenzene concentration according to

$$236 \quad -d[\text{nitrobenzene}]/dt = k_{\text{cells}} \times [\text{nitrobenzene}] \quad (1)$$

237 where  $k_{\text{cells}}$  is the first-order reduction rate constant ( $d^{-1}$ ) used  
238 to denote the rate by CN32-only;  $k_{\text{cells+clay}}$  is used to denote the  
239 first-order reduction rate constant by CN32 in the presence  
240 of iron-bearing clay minerals, and;  $k_{\text{clay}}$  is used to denote the  
241 first-order reduction rate constant by clay-Fe(II) in abiotic  
242 experiments.

243 To quantify electron transfer in our experiments, we calculated  
244 zero-order reaction rates normalized to electron equivalents.  
245 Reduction rates of nitrobenzene ( $R_{\text{NB}}$ ) and clay-Fe(III) ( $R_{\text{Fe}}$ )  
246 were calculated as ( $\mu\text{eq L}^{-1} \text{h}^{-1}$ )

$$247 \quad R_{\text{NB}} = 6 \times [\text{aniline}_t]/t \quad (2)$$

$$248 \quad R_{\text{Fe}} = ([\text{clay-Fe(II)}_t] - [\text{clay-Fe(II)}_0])/t \quad (3)$$

249 where  $[\text{aniline}_t]$  is the concentration of aniline at time  $t$  ( $\mu\text{M}$ ),  
250  $t$  is the length of the spike-period (h),  $[\text{clay-Fe(II)}_t]$  is the total  
251 Fe(II) concentration (HF-H<sub>2</sub>SO<sub>4</sub>/phenanthroline + soluble)  
252 at the end of the spike-period ( $\mu\text{M}$ ), and  $[\text{clay-Fe(II)}_0]$  is  
253 measured at the start of the spike-period ( $\mu\text{M}$ ). Zero-order rates  
254 were used because they fit the kinetics of both aniline and Fe(II)  
255 production (eqs 2 and 3, respectively) reasonably well over most  
256 of the spike-periods. Zero-order rates were also used to directly  
257 compare electron transfer to nitrobenzene versus clay-Fe(III) in  
258 biotic experiments, and electron transfer to nitrobenzene from

259 clay-Fe(II) in abiotic experiments. Reduction of nitrobenzene  
260 of aniline is known to be a six electron transfer process.<sup>32,47</sup>  
261 Therefore, electron equivalents were calculated by multiplying  
262 aniline concentrations and 6 e<sup>-</sup> per mol in eq 2. Aniline  
263 concentrations were used instead of nitrobenzene because they  
264 represented the final reduced product.

265 To quantitatively compare nitrobenzene reduction rates  
266 with and without an iron-bearing clay mineral, we define a "clay  
267 enhancement factor" as

$$\text{clay enhancement factor} = k_{\text{cells+clay}}/k_{\text{cells}} \quad (4) \quad 268$$

269 All statistical analyses were performed using IBM SPSS  
270 Statistics 20 (IBM Corp. NY).

## 271 ■ RESULTS AND DISCUSSION

272 **Biological Reduction of Nitrobenzene.** To test the role  
273 of iron-bearing clay minerals on the bioreduction of nitro-  
274 benzene by DMRB we used *Shewanella putrefaciens* CN32 to  
275 reduce (i) nitrobenzene in the presence/absence of iron-  
276 bearing clay minerals and (ii) iron-bearing clay minerals in the  
277 presence/absence of nitrobenzene. We found that *Shewanella*  
278 *putrefaciens* CN32 concurrently reduced both nitrobenzene  
279 and clay-Fe(III) (Figure 1a,d,g). After the first spike of  
280 nitrobenzene (Spike 1 in Figure 1), the first-order rate constant  
281 for nitrobenzene reduction ( $k_{\text{cell}}$ ) was  $1.31 \pm 0.01 \text{ d}^{-1}$  in the  
282 absence of clay, and increased to  $1.88 \pm 0.05 \text{ d}^{-1}$  and  $1.53 \pm$   
283  $0.01 \text{ d}^{-1}$  in the presence of montmorillonite SWy-2 and  
284 nontronite NAu-2 ( $k_{\text{cells+clay}}$ ), respectively (Figure 1a, Table 1).  
285 Both SWy-2 and NAu-2 significantly ( $P < 0.01$ ) enhanced the  
286 kinetics of nitrobenzene reduction. Nitrobenzene reduction  
287 rates in the presence of Al<sub>2</sub>O<sub>3</sub> were not significantly different  
288 from results obtained with CN32 alone ( $P > 0.1$ ; SI Figure S2).  
289 This result indicated that the enhancement of nitrobenzene  
290 reduction by iron-bearing clay minerals was not solely  
291 attributed to the presence of a mineral surface, and that  
292 iron(II) in clay minerals likely played an important role in the  
293 enhancement of nitrobenzene reduction. Sorption of nitro-  
294 benzene to the clay minerals or Al<sub>2</sub>O<sub>3</sub> did not account for more  
295 than 1% of the added mass of nitrobenzene in any of the  
296 experiments.

297 The clay enhancement factors (eq 4) were greater than one  
298 for both SWy-2 and NAu-2 and increased over time. The  
299 increased rate of nitrobenzene reduction in the presence of  
300 iron-bearing clay minerals was driven by biogenic clay-Fe(II).  
301 Nitrobenzene and clay-Fe(III) did not become competitive  
302 electron acceptors because excess electron donor was  
303 provided.<sup>32</sup> The production of biogenic clay-Fe(II) then  
304 promoted the abiotic reduction of nitrobenzene. We hypothe-  
305 sized that clay-Fe(II)-mediated reduction would become  
306 increasingly important with the accumulation of biogenic  
307 clay-Fe(II). To test this, we respiked nitrobenzene into the  
308 reactors two additional times (Spike 2 at  $t = 45 \text{ h}$ , Spike 3 at  
309  $t = 500 \text{ h}$ ). These experiments allowed us to assess how  
310 nitrobenzene fate was affected by extended incubation times  
311 and increased clay-Fe(II) concentrations. Each nitrobenzene  
312 spike resulted in its rapid reduction (Figure 1a-c). For all three  
313 spikes and with both clay minerals we observed faster  
314 nitrobenzene reduction when the clay mineral was present  
315 relative to only CN32. The clay enhancement factors increased  
316 with each sequential spike of nitrobenzene for both clay  
317 minerals (SWy-2: Spike 1 =  $1.43 \pm 0.03$ , Spike 2 =  $1.89 \pm 0.04$ ,  
318 Spike 3 =  $2.49 \pm 0.14$ ; NAu-2: Spike 1 =  $1.17 \pm 0.01$ , Spike 2 =  $1.43 \pm 0.03$ , Spike 3 =  $2.49 \pm 0.14$ ).



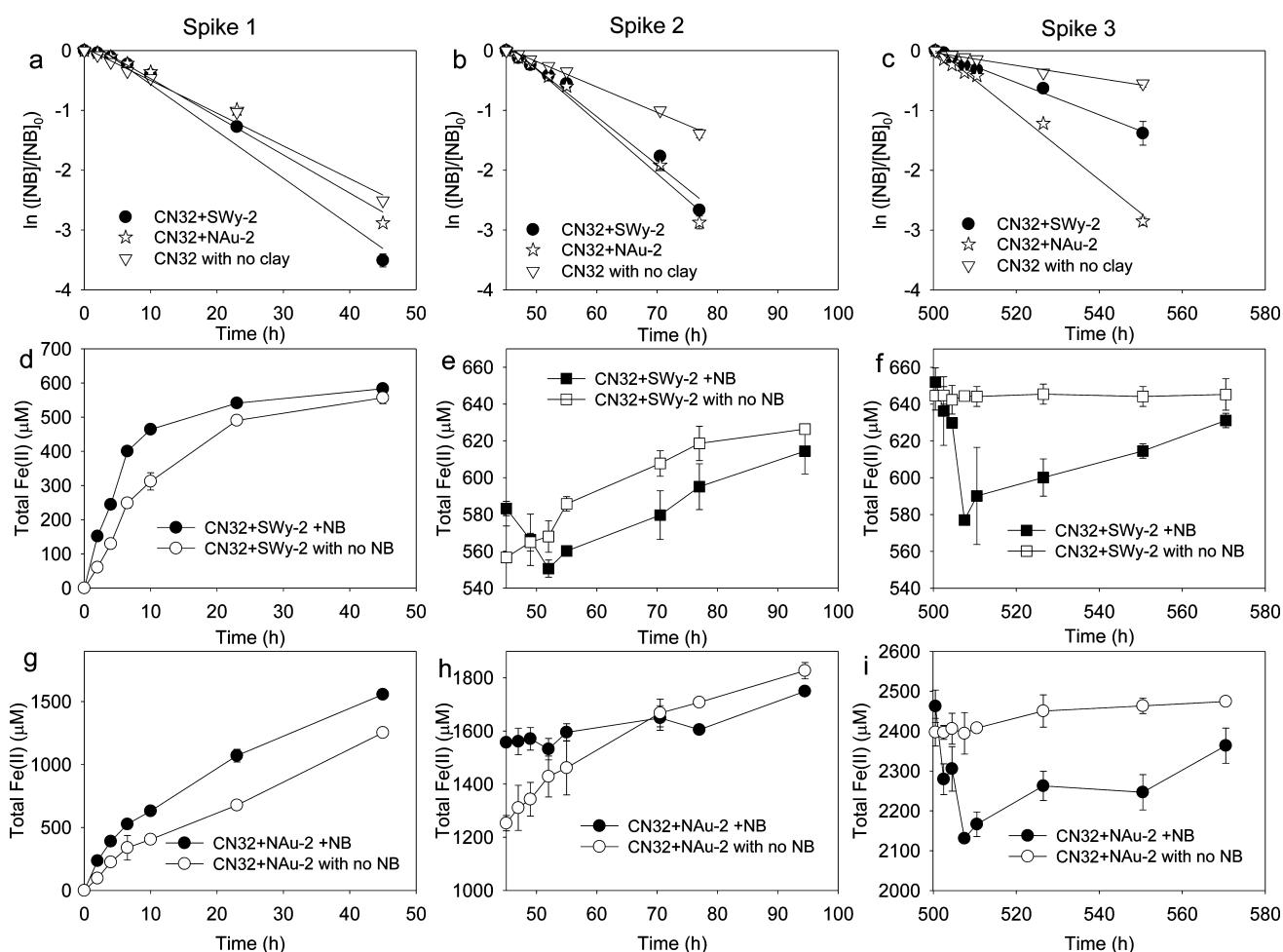


**Figure 1.** Biological reduction of nitrobenzene and iron-bearing clay minerals by *Shewanella putrefaciens* CN32. Experiments were initiated at  $t = 0$  h with  $210 \mu\text{M}$  nitrobenzene,  $1.0 \times 10^8$  cell  $\text{mL}^{-1}$  CN32, 10 mM lactate and  $\text{H}_2$  (2.5% headspace), and  $2.0 \text{ g L}^{-1}$  montmorillonite SWy-2 [ $0.78 \text{ mM}$  clay-Fe(III)] or  $2.0 \text{ g L}^{-1}$  nontronite NAu-2 [ $8.2 \text{ mM}$  clay-Fe(III)] in 10 mM PIPES buffer, pH 6.8. Nitrobenzene ( $250 \mu\text{M}$ ) was re-spiked into the reactors at  $t = 45$  h and  $t = 500$  h. (a–c)  $\ln([\text{nitrobenzene}]_t/[\text{nitrobenzene}]_0)$  versus time. (d–f) SWy-2 Fe(II) concentrations versus time. (g–i) NAu-2 Fe(II) concentrations versus time.

319 Spike 2 =  $2.05 \pm 0.05$ , Spike 3 =  $5.14 \pm 0.12$ ; Table 1), thus,  
320 confirming our hypothesis.

321 Measurements of clay-Fe(II) concentrations over time  
322 further confirmed the role that clay-Fe(II) played in this  
323 process. Clay-Fe(II) concentrations steadily increased over  
324 the first 45 h of the experiment (Figure 1d,g), increased more  
325 slowly from 45 to 100 h (Figure 1e,h), and then remained  
326 unchanged or declined from 100 to 550 h (Figure 1f,i). These  
327 data provided clear evidence that CN32 was simultaneously  
328 respiring on both clay-Fe(III) and nitrobenzene. Higher  
329 concentrations of clay-Fe(II) were measured in the presence  
330 of nitrobenzene as compared to the nitrobenzene-free controls  
331 in Spike 1 (Figure 1d,g), which was counterintuitive as one  
332 would expect clay-Fe(II) to be consumed via nitrobenzene  
333 reduction. We believe that this result was caused by an  
334 analytical interference in which intermediates in the nitro-  
335 benzene reduction process reduced Fe(III) during the acidic  
336 clay mineral digestion (SI Figure S3). This analytical  
337 interference was only an issue at the start of the experiments  
338 (Spike 1) when the clay-Fe(III) concentrations were highest,  
339 and became less important as clay-Fe(III) concentrations  
340 decreased (Spikes 2 and 3). At the longest incubation times,  
341 after Spike 3, clay-Fe(II) concentrations were systematically  
342 higher in the absence of nitrobenzene (Figure 1f,i). Since

nitrobenzene was the only oxidant present in the system, the  
343 drop in clay-Fe(II) was attributed to nitrobenzene reduction  
344 by clay-Fe(II).  
345

Mössbauer spectroscopy (MBS) was used to provide an  
346 additional measure of the extent of clay-Fe(III) reduction  
347 (Figure 2). Mössbauer spectra were collected for the biologically  
348 reduced minerals after 550 h of incubation to independently  
349 determine the clay-Fe(II) concentrations (Table 2). The values  
350 measured with Mössbauer spectroscopy were in reasonable  
351 agreement with those determined by HF- $\text{H}_2\text{SO}_4$ /phenanthroline  
352 digestion. Clay-Fe(II) concentrations measured by HF- $\text{H}_2\text{SO}_4$ /  
353 phenanthroline digestion were always higher than Fe(II) con-  
354 centrations measured by MBS, except for one partially chemically  
355 reduced NAu-2 sample. Fe(II) concentrations measured by  
356 HF- $\text{H}_2\text{SO}_4$ /phenanthroline digestion and MBS were in better  
357 agreement with NAu-2 versus SWy-2.  
358

**Electron Transfer Rates from CN32 to Nitrobenzene**  
359 **or Clay-Fe(III).** Electron transfer rates from CN32 to clay-  
360 Fe(III) ( $R_{\text{Fe}}$ ) and from CN32 to nitrobenzene ( $R_{\text{NB}}$ ) were  
361 compared by normalizing the rates to the number of electrons  
362 transferred (eqs 2 and 3). The rate of nitrobenzene reduction by  
363 CN32 (in the absence of a clay mineral) was  $25.5 \mu\text{eq L}^{-1} \text{ h}^{-1}$   
364 during Spike 1 (Table 1). The rate of clay-Fe(III) reduc-  
365 tion by CN32 (in the absence of nitrobenzene) was  
366

**Table 1. Summary of Pseudo-First-Order Rate Constants for Nitrobenzene Reduction and Zero-Order Rates for Electron Transfer Reactions with Combinations of *Shewanella putrefaciens* CN32, Nitrobenzene, and Montmorillonite SWy-2 or Nontronite NAu-2.<sup>a</sup>**

reaction description	experimental components		first-order rate constants			electron transfer rates			
	nitrobenzene (μM) <sup>b</sup>	SWy-2 (g L <sup>-1</sup> )/clay-Fe(III) (mM)	NAu-2 (g L <sup>-1</sup> )/clay-Fe(III) (mM)	spike 1 0–45 h	spike 2 45–77 h	spike 3 500–550 h	spike 1 0–45 h	spike 2 45–77 h	spike 3 500–550 h
nitrobenzene bioreduction	210–250	0/0	0/0	1.31 ± 0.01 (0.990)	1.02 ± 0.04 (0.995)	0.259 ± 0.03 (0.978)	25.5	33.9	10.5
nitrobenzene reduction with SWy-2	210–250	2.0/0.78	0/0	1.88 ± 0.05 (0.977)	1.93 ± 0.01 (0.982)	0.646 ± 0.05 (0.992)	27.8	38.9	18.7
nitrobenzene reduction with NAu-2	210–250	0/0	2.0/8.2	1.53 ± 0.01 (0.973)	2.10 ± 0.05 (0.983)	1.33 ± 0.04 (0.989)	26.1	41.9	24.6
SWy-2 bioreduction	0	2.0/0.78	0/0						
NAu-2 bioreduction	0	0/0	2.0/8.2				12.4	1.94	0.012

<sup>a</sup>All experiments conducted with 1 × 10<sup>8</sup> cells mL<sup>-1</sup> CN32 and 10 mM lactate in 10 mM PIPES, pH 6.8. <sup>b</sup>[Nitrobenzene]<sub>0</sub> = 210 μM at start of Spike 1. [nitrobenzene]<sub>0</sub> = 250 μM at starts of Spikes 2 and 3. <sup>c</sup>Regression slope ± 95% confidence interval. <sup>d</sup>R<sup>2</sup> for regression of ln([nitrobenzene]<sub>t</sub>/[nitrobenzene]<sub>0</sub>) versus time of spike-period.

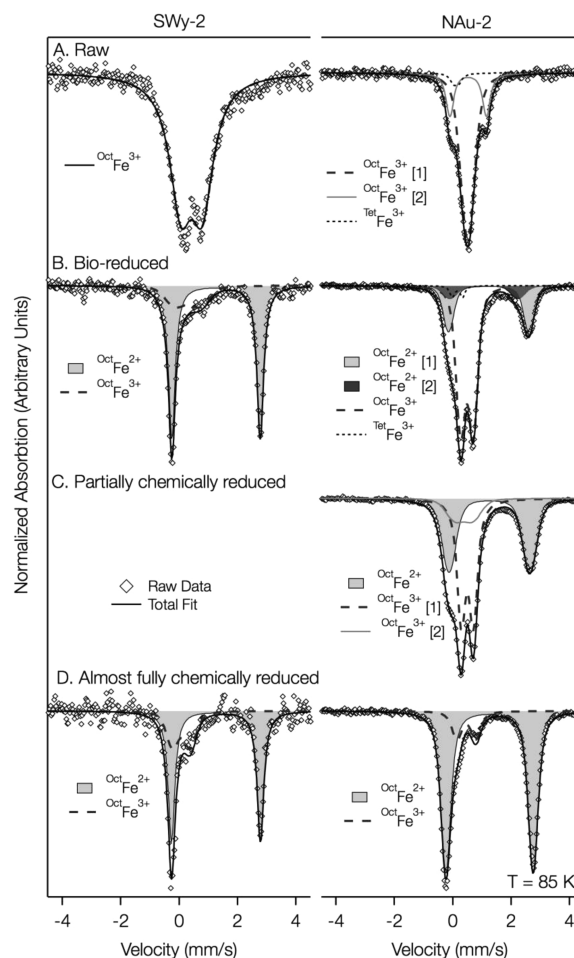


**Figure 2.** <sup>57</sup>Fe Mössbauer spectra collected for the native, biologically reduced and chemically reduced SWy-2 and NAu-2 samples at 85 °K. Oct-Fe<sup>3+</sup> = octahedral Fe(III), Tet-Fe<sup>3+</sup> = tetrahedral Fe(III), and Oct-Fe<sup>2+</sup> = octahedral Fe(II). Bracketed numbers shown after site assignments indicate that multiple distinct sites were found for the phase. Fitted hyperfine parameters and relative areas of each site are provided in Table 2.

12.4 μeq L<sup>-1</sup> h<sup>-1</sup> for SWy-2 and 27.8 μeq L<sup>-1</sup> h<sup>-1</sup> for NAu-2. The similarity between the values for nitrobenzene and clay-Fe(III) at nearly identical rates suggested that CN32 could respire on nitrobenzene and clay-Fe(III) at nearly identical rates. The lower rate for SWy-2 relative to NAu-2 was due to the smaller amount of clay-Fe(III) in SWy-2.

Over longer incubation periods (Spikes 2 and 3 in Figure 1), CN32 reduced clay-Fe(III) at rates slower than for nitrobenzene (i.e., R<sub>NB</sub> ≫ R<sub>Fe</sub>; Table 1). This was likely due to only a fraction of the remaining clay-Fe(III) being reducible due to biological accessibility and/or thermodynamic constraints. Negative values for R<sub>Fe</sub> during Spike 3 reflected the consumption of clay-Fe(II) coupled to nitrobenzene reduction. The reduction of nitrobenzene by clay-Fe(II) contributed to the high clay enhancement factors measured during Spike 3.

**Abiotic Reduction of Nitrobenzene.** In abiotic experiments, nitrobenzene was reduced by both bioreduced SWy-2 and bioreduced NAu-2 (Figure 3a,b). We found good stoichiometric agreement between 6 mol of Δclay-Fe(II) produced per 1 mol of Δaniline produced (Figure 3c). These results confirmed that Fe(III)-bearing clay minerals enhanced

Table 2. Mössbauer Spectroscopy (MBS) Fitted Hyperfine Parameters for Spectra Shown in Figure 2<sup>a</sup>

sample	CS, mm/s	QS, mm/s	phase	RA (%)	%Fe(II) by MBS	%Fe(II) by HF-H <sub>2</sub> SO <sub>4</sub> /phenanthroline
unaltered SWy-2	0.42	0.74	octahedral clay-Fe(III)	100.0	0	2.70
biologically reduced SWy-2	1.26	3.03	octahedral clay-Fe(II)	77.2	77.2	90.0
	0.27	0.87	octahedral clay-Fe(III)	22.8		
chemically reduced SWy-2	1.26	3.05	octahedral clay-Fe(II)	71.0	71.0	90.9
	0.07	0.61	octahedral clay-Fe(III)	29.0		
unaltered NAu-2	0.51	0.28	octahedral clay-Fe(III)	71.9	0	0.60
	0.52	1.25	octahedral clay-Fe(III) [2]	23.7		
	0.11	0.18	tetrahedral clay-Fe(III)	4.4		
biologically reduced NAu-2	1.06	2.33	octahedral clay-Fe(II)	8.5	32.3	34.5
	1.23	2.75	octahedral clay-Fe(II) [2]	23.8		
	0.48	0.44	octahedral clay-Fe(III)	64.5		
	0.16	0.35	tetrahedral clay-Fe(III)	3.2		
partially chemically reduced NAu-2	1.20	2.59	octahedral clay-Fe(II)	20.8	42.0	38.0
	1.27	2.96	octahedral clay-Fe(II) [2]	21.2		
	0.49	0.43	octahedral clay-Fe(III)	54.9		
	0.21	0.38	tetrahedral clay-Fe(III)	3.1		
chemically reduced NAu-2	1.26	2.99	octahedral clay-Fe(II)	85.5	85.5	91.1
	0.47	0.65	octahedral clay-Fe(III)	14.5		

<sup>a</sup> All spectra were collected at  $T = 85$  °K. CS = center shift, QS = quadrupole split, and RA = relative phase abundance in %. Site assignments were done comparing the fitted hyperfine parameters to known ranges for clay-Fe (<http://www.amazon.com/Mössbauer-Spectroscopy-Environmental-Industrial-Utilization/dp/1402077262>).

nitrobenzene reduction due to the formation and reaction of clay-Fe(II).

Prior work has shown that biological and chemical reduction of clay minerals can yield spectroscopically different clay mineral products—as determined by Mössbauer spectra collected at 4 °K.<sup>40</sup> Here we used Mössbauer spectroscopy at 85 °K to compare biologically- and chemically reduced specimens of SWy-2 and NAu-2 (Figure 2). Characterization of both minerals in their native redox-state indicated that both minerals contained only Fe(III), within detection limits (~1%). SWy-2 contained only octahedrally coordinated Fe(III) while NAu-2 contained mostly octahedral Fe(III) (96%) with a small amount of tetrahedral Fe(III) (4%). The spectra were consistent with previously published data.<sup>4</sup> For SWy-2, the biologically- and chemically reduced specimens were virtually identical, containing both octahedral Fe(III) and octahedral Fe(II) (Figure 2, left: B,D). The slight differences in relative areas of the Fe(II) and Fe(III) doublets can be attributed to challenges in controlling the extent of reduction using dithionite. For NAu-2, however, spectral variations were observed, particularly for the structural Fe(II) (Figure 2, right: B,C). The spectrum of biologically reduced NAu-2 was best fit using two Fe(II) doublets, both characteristic of octahedral Fe(II) in a clay mineral.<sup>48,49</sup> The spectrum of chemically reduced NAu-2 was best fit using only one Fe(II) doublet, suggesting that the local binding environment of Fe(II) in NAu-2 varied between the two reduced samples.

Even though it is difficult to correlate spectroscopic differences to reactivity<sup>50</sup> (e.g., since coexisting factors can influence fit parameters<sup>51–55</sup>), we found that chemically reduced iron-bearing clay minerals reduced nitrobenzene more rapidly than biologically reduced iron-bearing clay minerals (Figure 3, Table 3). At near-equal clay-Fe(II) concentrations and essentially equal reduction extents, dithionite-reduced SWy-2 [1.1 mM clay-Fe(II), 91% Fe(II)] reduced nitrobenzene faster ( $k_{\text{clay}} = 0.0117 \text{ d}^{-1}$ ,  $R_{\text{NB}} = 0.680 \mu\text{eq L}^{-1} \text{ h}^{-1}$ ) as compared to biologically reduced SWy-2 (1.3 mM clay-Fe(II), 90% Fe(II);

$k_{\text{clay}} = 0.00770 \text{ d}^{-1}$ ,  $R_{\text{NB}} = 0.324 \mu\text{eq L}^{-1} \text{ h}^{-1}$ ). Similar results were obtained with NAu-2. At near-equal clay-Fe(II) concentrations and reduction extents, dithionite-reduced NAu-2 (5.1 mM clay-Fe(II), 38% Fe(II), 3.3 g L<sup>-1</sup>) reduced nitrobenzene faster ( $k_{\text{clay}} = 0.0934 \text{ d}^{-1}$ ,  $R_{\text{NB}} = 3.41 \mu\text{eq L}^{-1} \text{ h}^{-1}$ ) as compared to biologically reduced NAu-2 (5.3 mM clay-Fe(II), 35% Fe(II), 3.7 g L<sup>-1</sup>;  $k_{\text{clay}} = 0.0326 \text{ d}^{-1}$ ,  $R_{\text{NB}} = 1.79 \mu\text{eq L}^{-1} \text{ h}^{-1}$ ).

We also found that chemically reduced NAu-2 reduced nitrobenzene faster as compared to chemically reduced SWy-2 (Table 3). Because SWy-2 (0.40 mmol Fe/g) and NAu-2 (4.1 mmol Fe/g) contain different amounts of Fe and are biologically reduced to different extents, abiotic experiments were conducted with clay minerals that had been chemically reduced to the same extent. At equal clay-Fe(II) concentrations [1.1 mM clay-Fe(II)] and equal reduction extents [91% Fe(II)], dithionite-reduced NAu-2 reduced nitrobenzene faster ( $k_{\text{clay}} = 0.0139 \text{ d}^{-1}$ ,  $R_{\text{NB}} = 0.757 \mu\text{eq L}^{-1} \text{ h}^{-1}$ ; Table 3) as compared to dithionite-reduced SWy-2 ( $k_{\text{clay}} = 0.0117 \text{ d}^{-1}$ ,  $R_{\text{NB}} = 0.680 \mu\text{eq L}^{-1} \text{ h}^{-1}$ ; Table 3). The faster nitrobenzene reduction kinetics were measured even with a 10-fold lower clay suspension used with the dithionite-reduced NAu-2 (0.31 g/L) as compared to dithionite-reduced SWy-2 (3.1 g/L). The different reactivity of SWy-2 versus NAu-2 may have been caused by the different types of structural Fe(II) in these clay minerals (Table 2).<sup>22,37</sup>

The different reactivity of SWy-2 versus NAu-2 toward nitrobenzene may also have been caused by the different reduction potentials ( $E_{\text{h}}$ ) of these clay minerals. Recently, our group developed a mediated electrochemical technique to measure reduction potential values for structural Fe in clay minerals as a function of Fe(II)/Total<sub>Fe</sub>.<sup>4,50</sup> These measurements provided the redox profile distributions to relate the percentage of structural Fe(II) to  $E_{\text{h}}$ .<sup>50</sup> From the redox profile distributions for SWy-2 and NAu-2, we found that 91% Fe(II) dithionite-reduced NAu-2 has a more negative reduction potential ( $E_{\text{h}} \approx -0.53 \text{ V}$ ) than 91% Fe(II) dithionite-reduced SWy-2

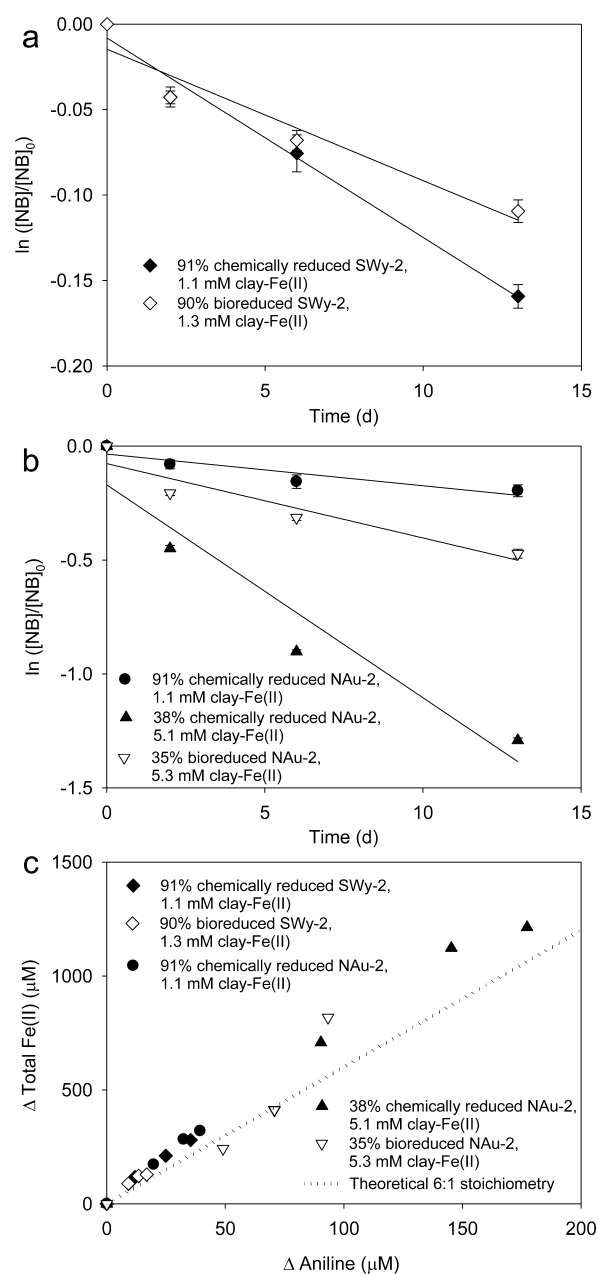


**Figure 3.** Abiotic reduction of nitrobenzene by biologically reduced and chemically reduced iron-bearing clay minerals. (a) Montmorillonite SWy-2. (b) Nontronite NAu-2. (c) Stoichiometric relationships between  $\Delta$  mol Fe(II) and  $\Delta$  mol aniline for the different clay-Fe(II) measurements. Dashed line represents theoretical stoichiometry of 6  $\Delta$  mol Fe(II) to 1  $\Delta$  mol aniline.

( $E_h \approx -0.29$  V). Our results imply that the  $E_h$  of iron-bearing clay minerals may influence their reaction rates with NACs.

**Environmental Significance.** We believe this is the first study demonstrating that iron-bearing clay minerals can enhance the bioreduction of nitrobenzene. In our previous study with hematite, nitrobenzene and DMRB, we showed that hematite could enhance the bioreduction of nitrobenzene.<sup>35</sup> Incubation periods in that study were relatively short (<24 h) such that direct bacterial reduction of nitrobenzene was far more important than indirect reduction by biogenic Fe(II). In our current study, however, we show that indirect contaminant reduction by biogenic clay-Fe(II) becomes much more important as the incubation period increases (>500 h). The reactivity in these long-term incubations may better represent environmental systems that have been reduced slowly and for a long time (e.g., aquifers contaminated with organic pollutants). While Fe(II) produced via bioreduction of Fe(III) oxides may be transported out of an aquifer, biogenic clay-Fe(II) would remain as an important redox-active component.

We also believe this is the first study demonstrating that biologically reduced iron-bearing clay minerals are less reactive than chemically reduced iron-bearing clay minerals toward nitrobenzene. While the reason for this difference is unresolved, it is consistent with spectroscopic studies showing structural differences that depend upon the reduction pathway<sup>40</sup> and with our own Mössbauer spectroscopy results (Figure 2, Table 2). A companion study has been completed to characterize the reactivity of biologically reduced iron-bearing clay minerals toward NACs.<sup>56</sup> Because most contaminated aquifers become reduced via biological activity, the reactivity of biogenic clay-Fe(II) toward reducible contaminants is particularly important.

## ■ ASSOCIATED CONTENT

### 📄 Supporting Information

Figure S1. Bioreduction of Fe-bearing clay minerals by *Shewanella putrefaciens* CN32 in the presence of aniline or methanol. Figure S2. Pseudo-first-order reduction rates during bioreduction of nitrobenzene in the presence of NAu-2, SWy-2 and Al<sub>2</sub>O<sub>3</sub>. Figure S3. Analytical interference of clay-Fe(II) measurement by nitrosobenzene. This material is available free of charge via the Internet at <http://pubs.acs.org>.

## ■ AUTHOR INFORMATION

### Corresponding Author

\*William D. Burgos, Dept. of Civil and Environmental Engineering, The Pennsylvania State University, 212 Sackett Building, University Park, PA, 16802 phone: 814-863-0578; fax: 814-863-7304. Email: [wdb3@psu.edu](mailto:wdb3@psu.edu).

**Table 3. Summary of Pseudo-First-Order Rate Constants and Zero-Order Rates for the Abiotic Reduction of Nitrobenzene by Biologically-Reduced or Chemically-Reduced Montmorillonite SWy-2 or Nontronite NAu-2.<sup>a</sup>**

clay-Fe(II) description	SWy-2 (g L <sup>-1</sup> )/clay-Fe(II) (mM)	NAu-2 (g L <sup>-1</sup> )/clay-Fe(II) (mM)	first-order rate constant ( $R^2$ ) <sup>c</sup> $k_{\text{clay}}$ (d <sup>-1</sup> ) <sup>b</sup>	zero-order rate $R_{\text{NB}}$ ( $\mu\text{eq L}^{-1} \text{h}^{-1}$ )
90% biologically reduced SWy-2	3.6/1.3	0/0	0.00770 ± 0.0004 (0.928)	0.324
91% chemically reduced SWy-2	3.1/1.1	0/0	0.0117 ± 0.002 (0.986)	0.680
35% biologically reduced NAu-2	0/0	3.7/5.3	0.0326 ± 0.001 (0.893)	1.79
38% chemically reduced NAu-2	0/0	3.3/5.1	0.0934 ± 0.003 (0.920)	3.41
91% chemically reduced NAu-2	0/0	0.31/1.1	0.0139 ± 0.001 (0.852)	0.757

<sup>a</sup>All experiments conducted with [nitrobenzene]<sub>0</sub> = 250  $\mu\text{M}$  in 50 mM PIPES, pH 6.8. <sup>b</sup>Regression slope  $\pm$ 95% confidence interval. <sup>c</sup> $R^2$  for regression of  $\ln([NB]_t/[NB]_0)$  versus time (0–13 d).



509 **Notes**

510 The authors declare no competing financial interest.

511 ■ **ACKNOWLEDGMENTS**

512 This research was supported by the Subsurface Biogeochemical  
513 Research (SBR) Program, Office of Science (BER), U.S.  
514 Department of Energy (DOE) grant no. DE-SC0005333 to  
515 The Pennsylvania State University.

516 ■ **REFERENCES**

517 (1) Favre, F.; Stucki, J. W.; Boivin, P. Redox properties of structural  
518 Fe in ferruginous smectite. A discussion of the standard potential and  
519 its environmental implications. *Clays Clay Miner.* **2006**, *54* (4), 466–  
520 472.

521 (2) Stucki, J. W.; Lee, K.; Goodman, B. A.; Kostka, J. E. Effects of in  
522 situ biostimulation on iron mineral speciation in a sub-surface soil.  
523 *Geochim. Cosmochim. Acta* **2007**, *71* (4), 835–843.

524 (3) Komlos, J.; Peacock, A.; Kukkadapu, R. K.; Jaffe, P. R. Long-term  
525 dynamics of uranium reduction/reoxidation under low sulfate  
526 conditions. *Geochim. Cosmochim. Acta* **2008**, *72* (15), 3603–3615.

527 (4) Gorski, C. A.; Aeschbacher, M.; Soltermann, D.; Voegelin, A.;  
528 Baeyens, B.; Fernandes, M. M.; Hofstetter, T. B.; Sander, M. Redox  
529 properties of structural Fe in clay minerals. I. Electrochemical  
530 quantification of electron-donating and -accepting capacities of  
531 smectites. *Environ. Sci. Technol.* **2012**, *46* (17), 9360–9368.

532 (5) Coughlin, B. R.; Stone, A. T. Nonreversible adsorption of  
533 divalent metal-ions (Mn-II, Co-II Ni-II Cu-II and Pb-II) onto  
534 goethite—Effects of acidification, Fe-II Addition, and picolinic-acid  
535 addition. *Environ. Sci. Technol.* **1995**, *29* (9), 2445–2455.

536 (6) Jenne, E. A. Controls on Mn Fe Co Ni Cu and Zn concentrations  
537 in soils and water - significant role of hydrous Mn and Fe oxides. *Adv.*  
538 *Chem. Ser.* **1968**, *73*, 337–387.

539 (7) Lovley, D. R. Microbial Fe(III) reduction in subsurface  
540 environments. *Fems Microbiol. Rev.* **1997**, *20* (3–4), 305–313.

541 (8) Jickells, T. D.; An, Z. S.; Andersen, K. K.; Baker, A. R.;  
542 Bergametti, G.; Brooks, N.; Cao, J. J.; Boyd, P. W.; Duce, R. A.;  
543 Hunter, K. A.; Kawahata, H.; Kubilay, N.; laRoche, J.; Liss, P. S.;  
544 Mahowald, N.; Prospero, J. M.; Ridgwell, A. J.; Tegen, I.; Torres, R.  
545 Global iron connections between desert dust, ocean biogeochemistry,  
546 and climate. *Science* **2005**, *308* (5718), 67–71.

547 (9) Pollard, R. T.; Salter, I.; Sanders, R. J.; Lucas, M. I.; Moore, C.  
548 M.; Mills, R. A.; Statham, P. J.; Allen, J. T.; Baker, A. R.; Bakker, D. C.  
549 E.; Charette, M. A.; Fielding, S.; Fones, G. R.; French, M.; Hickman, A.  
550 E.; Holland, R. J.; Hughes, J. A.; Jickells, T. D.; Lampitt, R. S.; Morris,  
551 P. J.; Nedelec, F. H.; Nielsdotir, M.; Planquette, H.; Popova, E. E.;  
552 Poulton, A. J.; Read, J. F.; Seeyave, S.; Smith, T.; Stinchcombe, M.;  
553 Taylor, S.; Thomalla, S.; Venables, H. J.; Williamson, R.; Zubkov, M.  
554 V. Southern Ocean deep-water carbon export enhanced by natural iron  
555 fertilization. *Nature* **2009**, *457* (7229), 577–U581.

556 (10) Eglinton, T. I. Geochemistry A rusty carbon sink. *Nature* **2012**,  
557 *483* (7388), 165–166.

558 (11) Lalonde, K.; Mucci, A.; Ouellet, A.; Gelinas, Y. Preservation of  
559 organic matter in sediments promoted by iron. *Nature* **2012**, *483*  
560 (7388), 198–200.

561 (12) Riedel, T.; Zak, D.; Biester, H.; Dittmar, T. Iron traps  
562 terrestrially derived dissolved organic matter at redox interfaces. *Proc.*  
563 *Natl. Acad. Sci. U. S. A.* **2013**, *110* (25), 10101–10105.

564 (13) Borch, T.; Kretzschmar, R.; Kappler, A.; Van Cappellen, P.;  
565 Ginder-Vogel, M.; Voegelin, A.; Campbell, K. Biogeochemical redox  
566 processes and their impact on contaminant dynamics. *Environ. Sci.*  
567 *Technol.* **2010**, *44* (1), 15–23.

568 (14) Elsner, M.; Schwarzenbach, R. P.; Haderlein, S. B. Reactivity of  
569 Fe(II)-bearing minerals toward reductive transformation of organic  
570 contaminants. *Environ. Sci. Technol.* **2004**, *38* (3), 799–807.

571 (15) Gates, W. P.; Bouazza, A. Churchman G.J. Bentonite clay keeps  
572 pollutants at bay. *Elements* **2009**, *5* (2), 105–110.

573 (16) Anastacio, A. S.; Aouad, A.; Sellin, P.; Fabris, J. D.; Bergaya, F.;  
574 Stucki, J. W. Characterization of a redox-modified clay mineral with

respect to its suitability as a barrier in radioactive waste confinement. *575*  
*Appl. Clay Sci.* **2008**, *39* (3–4), 172–179. *576*

(17) Bishop, M. E.; Glasser, P.; Dong, H. L.; Arey, B.; Kovarik, L. *577*  
Reduction and immobilization of hexavalent chromium by Fe-bearing *578*  
clay minerals. *Abstr. Pap. Am. Chem. Soc.* **2013**, 246. *579*

(18) Brigatti, M. F.; Franchini, G.; Lugli, C.; Medici, L.; Poppi, L.; *580*  
Turci, E. Interaction between aqueous chromium solutions and layer *581*  
silicates. *Appl. Geochem.* **2000**, *15* (9), 1307–1316. *582*

(19) Fredrickson, J. K.; Zachara, J. M.; Kennedy, D. W.; Kukkadapu, *583*  
R. K.; McKinley, J. P.; Heald, S. M.; Liu, C. X.; Plymale, A. E. *584*  
Reduction of TcO<sub>4</sub><sup>-</sup> by sediment-associated biogenic Fe(II). *Geochim.* *585*  
*Cosmochim. Acta* **2004**, *68* (15), 3171–3187. *586*

(20) Bishop, M. E.; Dong, H. L.; Kukkadapu, R. K.; Liu, C. X.; *587*  
Edelmann, R. E. Bioreduction of Fe-bearing clay minerals and their *588*  
reactivity toward pertechnetate (Tc-99). *Geochim. Cosmochim. Acta* *589*  
**2011**, *75* (18), 5229–5246. *590*

(21) Yang, J. J.; Kukkadapu, R. K.; Dong, H. L.; Shelobolina, E. S.; *591*  
Zhang, J.; Kim, J. Effects of redox cycling of iron in nontronite on *592*  
reduction of technetium. *Chem. Geol.* **2012**, *291*, 206–216. *593*

(22) Neumann, A.; Hofstetter, T. B.; Lussi, M.; Cirpka, O. A.; Petit, *594*  
S.; Schwarzenbach, R. P. Assessing the redox reactivity of structural *595*  
iron in smectites using nitroaromatic compounds as kinetic probes. *596*  
*Environ. Sci. Technol.* **2008**, *42* (22), 8381–8387. *597*

(23) Hofstetter, T. B.; Neumann, A.; Schwarzenbach, R. P. Reduction *598*  
of nitroaromatic compounds by Fe(II) species associated with iron- *599*  
rich smectites. *Environ. Sci. Technol.* **2006**, *40* (1), 235–242. *600*

(24) Hofstetter, T. B.; Schwarzenbach, R. P.; Haderlein, S. B. *601*  
Reactivity of Fe(II) species associated with clay minerals. *Environ. Sci.* *602*  
*Technol.* **2003**, *37* (3), 519–528. *603*

(25) Neumann, A.; Hofstetter, T. B.; Skarpeli-Liati, M.; *604*  
Schwarzenbach, R. P. Reduction of polychlorinated ethanes and *605*  
carbon tetrachloride by structural Fe(II) in smectites. *Environ. Sci.* *606*  
*Technol.* **2009**, *43* (11), 4082–4089. *607*

(26) Schaefer, M. V.; Gorski, C. A.; Scherer, M. M. Spectroscopic *608*  
evidence for interfacial Fe(II)-Fe(III) electron transfer in a clay *609*  
mineral. *Environ. Sci. Technol.* **2011**, *45* (2), 540–545. *610*

(27) Gan, H.; Stucki, J. W.; Bailey, G. W. Reduction of structural Iron *611*  
in ferruginous smectite by free-radicals. *Clays Clay Miner.* **1992**, *40* (6), *612*  
659–665. *613*

(28) Pentrakova, L.; Su, K.; Pentrak, M.; Stuck, J. W. A review of *614*  
microbial redox interactions with structural Fe in clay minerals. *Clay* *615*  
*Miner.* **2013**, *48* (3), 543–560. *616*

(29) Dong, H. L.; Jaisi, D. P.; Kim, J.; Zhang, G. X. Microbe-clay *617*  
mineral interactions. *Am. Mineral.* **2009**, *94* (11–12), 1505–1519. *618*

(30) Padda, R. S.; Wang, C. Y.; Hughes, J. B.; Kutty, R.; Bennett, G. *619*  
N. Mutagenicity of nitroaromatic degradation compounds. *Environ.* *620*  
*Toxicol. Chem.* **2003**, *22* (10), 2293–2297. *621*

(31) Purohit, V.; Basu, A. K. Mutagenicity of nitroaromatic *622*  
compounds. *Chem. Res. Toxicol.* **2000**, *13* (8), 673–692. *623*

(32) Luan, F. B.; Burgos, W. D.; Xie, L.; Zhou, Q. Bioreduction of *624*  
nitrobenzene, natural organic matter, and hematite by *Shewanella* *625*  
*putrefaciens* CN32. *Environ. Sci. Technol.* **2010**, *44* (1), 184–190. *626*

(33) Zhu, Z. K.; Tao, L.; Li, F. B. 2-Nitrophenol reduction promoted *627*  
by *S. putrefaciens* 200 and biogenic ferrous iron: The role of different *628*  
size-fractions of dissolved organic matter. *J. Hazard. Mater.* **2014**, *279*, *629*  
436–443. *630*

(34) Luan, F.B.; Gorski, C. A.; Burgos, W. D. Thermodynamic *631*  
controls on the microbial reduction of iron-bearing nontronite and *632*  
uranium. *Environ. Sci. Technol.* **2014**, *48* (5), 2750–2758. *633*

(35) Zhang, G. X.; Senko, J. M.; Kelly, S. D.; Tan, H.; Kemner, K. M.; *634*  
Burgos, W. D. Microbial reduction of iron(III)-rich nontronite and *635*  
uranium(VI). *Geochim. Cosmochim. Acta* **2009**, *73* (12), 3523–3538. *636*

(36) McAllister, L. E.; Semple, K. T., Role of clay and organic matter *637*  
in the biodegradation of organics in soil. In *Geomicrobiology: Molecular* *638*  
*and Environmental Perspective*; Springer-Verlag: Berlin, Berlin, 2010; pp *639*  
367–384. *640*

(37) Neumann, A.; Petit, S.; Hofstetter, T. B. Evaluation of redox- *641*  
active iron sites in smectites using middle and near infrared *642*  
spectroscopy. *Geochim. Cosmochim. Acta* **2011**, *75* (9), 2336–2355. *643*



- 644 (38) Gorski, C. A.; Scherer, M. M. *Fe<sup>2+</sup> Sorption at the Fe Oxide-Water*  
645 *Interface: A Revised Conceptual Framework, Aquatic Redox Chemistry*;  
646 American Chemical Society: WA, 2011; pp 315–343.
- 647 (39) Ernstsen, V.; Gates, W. P.; Stucki, J. W. Microbial reduction of  
648 structural iron in clays—A renewable source of reduction capacity. *J.*  
649 *Environ. Qual.* **1998**, *27* (4), 761–766.
- 650 (40) Ribeiro, F. R.; Fabris, J. D.; Kostka, J. E.; Komadel, P.; Stucki, J.  
651 W. Comparisons of structural iron reduction in smectites by bacteria  
652 and dithionite: II. A variable-temperature Mossbauer spectroscopic  
653 study of Garfield nontronite. *Pure Appl. Chem.* **2009**, *81* (8), 1499–  
654 1509.
- 655 (41) Royer, R. A.; Burgos, W. D.; Fisher, A. S.; Unz, R. F.; Dempsey,  
656 B. A. Enhancement of biological reduction of hematite by electron  
657 shuttling and Fe(II) complexation. *Environ. Sci. Technol.* **2002**, *36* (9),  
658 1939–1946.
- 659 (42) Keeling, J. L.; Raven, M. D.; Gates, W. P. Geology and  
660 characterization of two hydrothermal nontronites from weathered  
661 metamorphic rocks at the Uley Graphite Mine, South Australia. *Clay*  
662 *Clay Miner.* **2000**, *48* (5), 537–548.
- 663 (43) Luan, F. B.; Burgos, W. D. Sequential extraction method for  
664 determination of Fe(II/III) and U(IV/VI) in suspensions of iron-  
665 bearing phyllosilicates and uranium. *Environ. Sci. Technol.* **2012**, *46*  
666 (21), 11995–12002.
- 667 (44) Stucki, J. W.; Golden, D. C.; Roth, C. B. Preparation and  
668 handling of dithionite-reduced smectite suspensions. *Clay Clay Min.*  
669 **1984**, *32* (3), 191–197.
- 670 (45) Jaisi, D. P.; Dong, H. L.; Liu, C. X. Influence of biogenic Fe(II)  
671 on the extent of microbial reduction of Fe(III) in clay minerals  
672 nontronite, Illite, and chlorite. *Geochim. Cosmochim. Acta* **2007**, *71* (5),  
673 1145–1158.
- 674 (46) Stookey, L. L. Ferrozine—A new spectrophotometric reagent  
675 for iron. *Anal. Chem.* **1970**, *42* (7), 779–781.
- 676 (47) Klausen, J.; Trober, S. P.; Haderlein, S. B.; Schwarzenbach, R. P.  
677 Reduction of substituted nitrobenzenes by Fe(II) in aqueous mineral  
678 suspensions. *Environ. Sci. Technol.* **1995**, *29* (9), 2396–2404.
- 679 (48) Murad, E.; Cashion, J. *Mössbauer Spectroscopy of Environmental*  
680 *Materials and Their Industrial Utilization*; Kluwer Academic Publishers:  
681 Dordrecht, 2006.
- 682 (49) McCammon, C. Mössbauer spectroscopy of minerals. In  
683 *Mineral Physics and Crystallography: A Handbook of Physical Constants*;  
684 American Geophysical Union: Washington, D. C., 1995.
- 685 (50) Gorski, C. A.; Klupfel, L. E.; Voegelin, A.; Sander, M.;  
686 Hofstetter, T. B. Redox properties of structural Fe in clay minerals: 3.  
687 Relationships between smectite redox and structural properties.  
688 *Environ. Sci. Technol.* **2013**, *47* (23), 13477–13485.
- 689 (51) Dyar, M. D.; Agresti, D. G.; Schaefer, M. W.; Grant, C. A.;  
690 Sklute, E. C., Mossbauer spectroscopy of earth and planetary materials.  
691 In *Annual Review of Earth and Planetary Sciences*; Annual Reviews: Palo  
692 Alto, 2006; pp 83–125.
- 693 (52) Evans, R. J.; Rancourt, D. G.; Grodzicki, M. Hyperfine electric  
694 field gradients and local distortion environments of octahedrally  
695 coordinated Fe<sup>2+</sup>. *Am. Mineral.* **2005**, *90* (1), 187–198.
- 696 (53) Evans, R. J.; Rancourt, D. G.; Grodzicki, M. Hyperfine electric  
697 field gradient tensors at Fe<sup>2+</sup> sites in octahedral layers: Toward  
698 understanding oriented single-crystal Mössbauer spectroscopy meas-  
699 urements of micas. *Am. Mineral.* **2005**, *90* (10), 1540–1555.
- 700 (54) Rancourt, D. G. Mössbauer spectroscopy in clay sciences.  
701 *Hyperfine Interact.* **1998**, *117* (1–4), U7–U8.
- 702 (55) Cashion, J. D.; Gates, W. P.; Thomson, A. Mossbauer and IR  
703 analysis of iron sites in four ferruginous smectites. *Clay Miner.* **2008**,  
704 *43* (1), 83–93.
- 705 (56) Luan, F. B.; Gorski, C. A.; Burgos, W. D. Linear free energy  
706 relationships for the biotic and abiotic reduction of nitroaromatic  
707 compounds. *Environ. Sci. Technol.* **2014**, submitted.